Loss reduction in a windfarm participating in primary voltage control using an extension of the Convex DistFlow OPF

Benoît MARTIN
Philippe DE RUA
Emmanuel DE JAEGER
Mechatronic, Electrical Energy, and Dynamic Systems (MEED)
Institute of Mechanics, Materials and Civil Engineering (iMMC)
Université Catholique de Louvain (UCL)
Louvain-la-Neuve, Belgium
benoit.martin@uclouvain.be

François GLINEUR
Center for Operations Research and Econometrics (CORE)
Institute of Information and Communication Technologies, Electronics and Applied Mathematics (ICTEAM)
Université Catholique de Louvain (UCL)
Louvain-la-Neuve, Belgium

***Abstract*—One of the largest French onshore wind farms is requested by the transmission system operator (TSO) to participate in primary voltage control. This implies exchanging reactive power with the grid, by using both the wind turbines and static switchable capacitor and inductor banks installed in the windfarm. The reactive power setpoint dispatch between the wind turbines and the static units is currently suboptimal, leading to additional energy losses inside the collector grid of the wind farm. An extension of the Convex DistFlow OPF model accounting for real-network elements is presented in order to perform an optimal reactive dispatch minimizing energy losses on the collector grid. The proposed model is a Mixed-Integer Second Order Cone Program (MISOCP) that is further relaxed with an efficient linear outer approximation of conic constraints to alleviate the computational burden. This approach is then compared to a *Matpower*-based approach to assess its accuracy and computational efficiency on a wide range of operating conditions. The developed model exhibits a satisfying accuracy and outperforms *Matpower* on a significant fraction of tested cases.**

***Index Terms*—Convex optimization, Loss reduction, Optimal reactive dispatch, Wind farm**

I. Introduction

The 78 MW-wind farm considered in this paper participates in primary voltage control by injecting or absorbing reactive power at the point of common coupling (PCC), proportionally to the difference between the voltage at PCC and a voltage setpoint. For such a voltage static law, the reactive setpoint is limited by maximum capacitive and inductive values (Fig. 1). The reactive power is produced or consumed by the wind turbines (WTs) and by switchable static units installed at the MV busbar of the substation. Currently, the WTs are used first and the static units are only used in case of large reactive setpoints. In addition, the WTs receive equal reactive power setpoints, which might be suboptimal.

In this paper, the goal is to formulate the problem as an Optimal Power Flow (OPF) to optimally determine the tap at the on-load tap changer (OLTC) and the reactive power

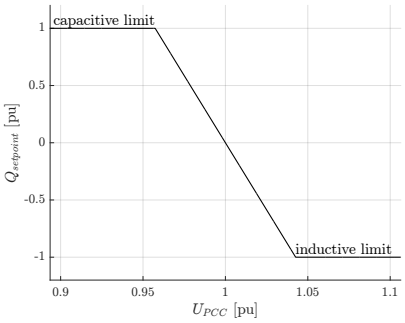


Fig. 1. Example of voltage static law

dispatch among the WTs and the static units. The objective is to reduce the active power losses in the transformers and cables of the wind farm while performing the primary voltage control.

The OPF problem consists in optimizing an objective, typically a function of active/reactive power injections, while satisfying both the AC power flow feasibility problem and engineering constraints related to equipment limits. The AC feasibility problem is known to be non-convex and is NP-hard even on radial networks [1]. The inclusion of integer decision variables linked to static units and OLTC operation makes the considered problem a Mixed-Integer Non-Linear Program (MINLP). Over the last decade, a significant body of literature has dealt with convex relaxations of this problem, ranging from Linear Programming (LP) to Semidefinite Programming (SDP) relaxations (see [2] for a complete survey on this topic). The NP-hardness of the problem implies that no tractable convex relaxation of the original problem may be exact. However, sets of sufficient conditions exist that guarantee the exactness of these formulations at the price of modifying the feasible space of the original problem which might not be suited for all OPF problems [2]. Regarding network modelling, most of the

convex relaxations do not deal with line charging capacitances, nor with transformers. Yet, in the present problem, the cables of the collector grid present a significant capacitive behavior, all wind turbines are connected through transformers and the transformer between the collector grid and the high voltage (HV) network is equipped with an OLTC. In [3], the authors propose a SDP formulation including shunt elements of lines as well as transformers. However, transformers are always operated at nominal tap ratio in this paper, and SDP formulations are practically intractable for real-world problems. In [4], the authors propose an exact Second Order Cone (SOCP) formulation including line charging capacitances where the feasibility set of the problem is slightly reduced by adding additional constraints. However, this formulation does not include transformers nor the operation of discrete assets (static units, OLTC).

In this paper, we base our approach upon the extended Convex DistFlow (CDF) model developed in [5] in which both the π model of lines and variable ratio transformers are considered. We extend it by including discrete models of OLTC and static unit banks switching. The resulting model can be cast as Mixed-Integer Second Order Cone (MISOCP), for which we give an efficient linear outer approximation (OA). We then assess the accuracy of this model in function of the degree of the OA, and we compare its performances to a non linear implementation of the problem using *Matpower* [6].

The paper is organised as follows: section II describes the problem at hand and the windfarm under study, section III describes the augmented model we propose for solving the problem, numerical results and comparison with *Matpower* are discussed in section IV before concluding in section V.

II. Problem description

The 78 MW wind farm comprises 39 DFIG-based wind turbines (WTs) grouped in 7 subparks. Transformers of 2.5 MVA connect the WTs to a 31 kV radial collector grid composed of buried cables. At the substation, a 120 MVA transformer equipped with an OLTC connects the 31 kV collector grid to the 235 kV transmission network.

Currently, the purpose of the OLTC is to maintain the voltage on the medium voltage (MV) side of the substation as close as possible to its rated value. The static units comprise three capacitor banks of $+5$ MVAR and three inductor banks of -5 MVAR. The reactive power capability of the WTs is defined by a capability curve in the PQ plane. Although the WTs can behave as loads in stand-by mode (i.e. consuming active power), they cannot produce nor consume reactive power for negative active power outputs, as displayed in Fig. 2. This is imposed beforehand by setting the maximum capacitive and inductive capabilities to zero for all the WTs with a negative active power output.

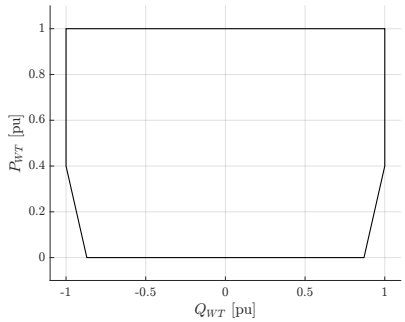


Fig. 2. Example of capability curve in the PQ space

III. Extended formulation of the Convex DistFlow Optimal Power Flow

The model we present hereunder is an extension of the one developed in [5]. The block of constraints A corresponds to the original formulation while blocks B and C are original contributions of the present paper.

A. Original formulation

The original formulation has been developed in order to tackle transmission network-related problems including transformers and for which line charging capacitances may not be neglected. In this model, branches are modelled in the same way as in *Matpower* (Fig. 3). More precisely, each branch is composed of an ideal transformer followed by a π-section line. This branch model, in combination with bus shunt admittances, allows to model non-ideal transformers ($b^c_{ij} = 0$) as well as simple line sections ($t_{ij} = 1$). The complete derivation of this model being beyond the scope of this paper, the interested reader is referred to [5] for more details.

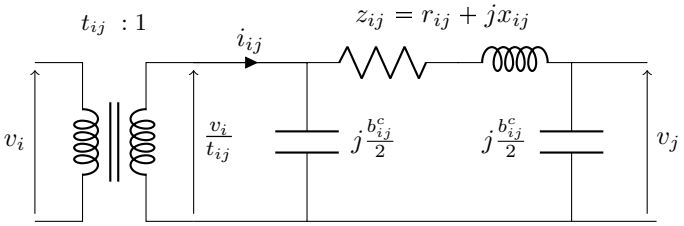


Fig. 3. *Matpower*-like line model

The objective to be minimized in this problem is composed of three terms. The first corresponds to the losses on the collector grid. Minimizing this term is equivalent to minimizing p_{PCC} (as p_{PCC} is negative if it is injected on the transmission network). The two other terms in the objective are penalty terms to be explained in subsection III-B.

The first set of constraints in the model (Block A) originates from [5]. Eqs. (1) and (2) represent the active and reactive power balance at every node of the network. Eqs. (3) and (4) model the active and reactive losses in the branches (lines and transformers) of the system and Eq. (5) represents the voltage drop on these branches. Eq. (6) represents the thermal rating limit for each branch. It is a second order cone (SOC) constraint, i.e. it defines a convex cone in $\mathbb{R}^3$ whose vertex is at the origin. Constraints (7) and (8) are linear inequalities

describing the capability curve of WTs displayed in Fig. 2. Note that no limit is imposed on active power output of WTs as it is considered as a parameter of the present problem. Eq. (9) is a relaxation of the constitutive equation $p_{ij}^2+q_{ij}^2 = \frac{w_i}{t_{ij}^2} l_{ij}$ linking power flows to voltage and current variables. It is a rotated SOC constraint that can be equivalently represented by two three-dimensional SOC constraints. Eq. (10) represents the voltage bounds at every node. Finally, constraints (11) and (12) model the limit on the voltage angle difference between two nodes.

It should be noted that two relaxations steps are made in this model: the SOC relaxation (9) and the convexification of the voltage drop equation that leads to (5). This convexification implies that voltage angles are not considered in the model anymore. However, in a radial setup (which is the case for the wind farm), angles can be recovered in a unique way from the solution as there are no cycles in the network, which would not be the case anymore in meshed networks. Hence, in this radial context, the relaxation is exact if and only if the right-hand term of (9) is equal to its left-hand term.

B. Point of common coupling

As mentioned above, the main transformer of the wind farm connects the collector grid to the PCC. Eqs. (13) and (14) model the power balance at the PCC while Eq. (15) models the transmission network voltage at the PCC. Eq. (16) models the fact that there might be a positive or negative mismatch between the reactive setpoint imposed to the wind farm and what the wind farm can actually produce/consume. Eqs. (17) and (18) impose that this mismatch is either positive or negative in a disjunctive way (big-M constraint, M being a suitable positive constant). The wind farm should follow the reactive setpoint if it is able to do so. Hence, we penalize $\nu\ (q_{mis}^+ + q_{mis}^-)$ in the minimization objective to avoid any reactive mismatch if there is no need for it. Finally, Eqs. (19) and (20) represent the activation of the static unit banks. Eq. (19) states that only a single state can be chosen for these units. Eq. (20) is a big-M constraint that represents the reactive power exchange with the static units in function of their state in a disjunctive way.

C. On-load tap changer

The main transformer of the wind farm, connecting the collector grid to the transmission network, is equipped with an OLTC that allows to modify the turns ratio of this transformer by discrete increments/decrements in a certain range around its nominal value. Eq. (21) models the fact that only one tap may be chosen at a given time. Eqs. (22) and (23) are the equivalent of eqs. (3) and (4) for the OLTC, written as a big-M constraint to account for the discrete nature of the tap changer while keeping convexity. Similarly, Eq. (25) is the big-M equivalent of (9) for the OLTC. For sake of brevity, the computation of M values in big-M constraints is not detailed in this paper. However, the underlying rationale is to choose the lowest possible value of M such that the corresponding constraint is not binding when the considered binary variable (σ, τ) is equal to 0, in order to keep the model as tight as possible.

SYMBOL DEFINITIONS

A. Sets

N	The set of nodes in the network
E	The set of directed arcs representing the lines in the network
E^R	The set of lines in E taken in the opposite direction

B. Parameters

n_{taps}	Amount of taps for the OLTC
n_{banks}	Amount of poss. states for the static unit banks
$r_{s,OLTC}^k, x_{s,OLTC}^k$	Series elements of the OLTC at k^{th} tap
t_{OLTC}^k	Turns ratio of the OLTC for the k^{th} tap
p_i^g	Measured active power produced by the wind turbine at node i
v_{PCC}	Voltage at the point of common coupling
$q_{PCC}^{set} = f(v_{PCC})$	Reactive power exchange at PCC, fixed by the droop characteristic of the plant
$y_i^s = g_i^s + \boldsymbol{j} b_i^s$	Shunt admittance at node i
b_{bank}^k	Equivalent shunt susceptance of the static unit banks for the k^{th} state
b_{ij}^c	Line charging susceptance of the π model of the line between nodes i and j
$z_{ij} = r_{ij} + \boldsymbol{j} x_{ij}$	Impedance of the line between i and j
$t_{ij} = t_{ij}^R + \boldsymbol{j} t_{ij}^I$	Turns ratio of the transformer located between i and j, in rectangular form
$tz_{ij}^{*R} = r_{ij} t_{ij}^R + x_{ij} t_{ij}^I$	
$tz_{ij}^{*I} = r_{ij} t_{ij}^I - x_{ij} t_{ij}^R$	
θ^Δ	Max. phase angle diff. between 2 nodes
$\overline{s}_{ij}$	Line thermal limit
$\underline{v}_i, \overline{v}_i$	Lower and upper voltage bounds at i
$\underline{q}, \overline{q}, q_{sl}^-, q_{sl}^+, q^0$	Constants for the WTS capability curve
ν	Weight for the reactive mismatch in the objective

C. Variables

p_{PCC}	Active power exchange at PCC, $\leqslant 0$ (resp. $\geqslant 0$) if injected on (resp. drawn from) the grid
q_{PCC}	Idem for reactive power
$q_{mis}^+, q_{mis}^- \geqslant 0$	Mismatch with the reactive setpoint if $q_{PCC} \geqslant 0$ (q_{mis}^+) or $q_{PCC} \leqslant 0$ (q_{mis}^-)
μ	Binary representing whether the reactive mismatch is positive or negative
$\dot{\sim}$	Vector quantity notation.
i_{ij}	Current $\forall (i,j) \in E$
v_i	Voltage $\forall i \in N$
$l_{ij} = \lvert i_{ij} \rvert^2$	$\forall (i,j) \in E$
$w_i = \lvert v_i \rvert^2$	$\forall i \in N$
p_{ij}	Active power flow $\forall (i,j) \in E \cup E^R$
q_{ij}	Reactive power flow $\forall (i,j) \in E \cup E^R$
q_i^g	Reactive power generation/consumption $\forall i \in N$
τ^k	Binary, = 1 if tap k is chosen $k \in \{1, ..., n_{taps}\}$
σ^k	Binary, = 1 if static unit bank state k is chosen $k \in \{1, ..., n_{banks}\}$

Model : Extended CDF-OPF for wind farm loss reduction

minimize: $p_{PCC} + \nu \left(q^{+}_{mis} + q^{-}_{mis}\right)$

subject to:

A. Lines, transformers and nodes of the collector grid

$$p^g_i - g^s_i w_i = \sum_{(i,j)\in E\cup E^R} p_{ij} \tag{1}$$

$$q^g_i + b^s_i w_i = \sum_{(i,j)\in E\cup E^R} q_{ij} \tag{2}$$

$$p_{ij} + p_{ji} = r_{ij}\left(l_{ij} + b^c_{ij}q_{ij} + \left(\frac{b^c{}_{ij}}{2}\right)^2 \frac{w_i}{t^2_{ij}}\right) \tag{3}$$

$$q_{ij} + q_{ji} = x_{ij}\left(l_{ij} + b^c_{ij}q_{ij} + \left(\frac{b^c_{ij}}{2}\right)^2 \frac{w_i}{t^2_{ij}}\right) - \frac{b^c_{ij}}{2}\left(\frac{w_i}{t^2_{ij}} + w_j\right) \tag{4}$$

$$\left(1 - x_{ij}b^c_{ij}\right)\frac{w_i}{t^2_{ij}} - w_j = 2(r_{ij}p_{ij} + x_{ij}q_{ij})$$

$$-\left(r^2_{ij} + x^2_{ij}\right)\left(l_{ij} + b^c_{ij}q_{ij} + \left(\frac{b^c_{ij}}{2}\right)^2 \frac{w_i}{t^2_{ij}}\right) \tag{5}$$

$$p^2_{ij} + q^2_{ij} \leqslant (\overline{s}_{ij})^2 \tag{6}$$

$$\underline{q} \leqslant q^g_i \leqslant \overline{q} \tag{7}$$

$$-q^0 - q^-_{sl}p^i_g \leqslant q^g_i \leqslant q^0 + q^+_{sl}p^i_g \tag{8}$$

$$p^2_{ij} + q^2_{ij} \leqslant \frac{w_i}{t^2_{ij}} l_{ij} \tag{9}$$

$$(\underline{v}_i)^2 \leqslant w_i \leqslant (\overline{v}_i)^2 \tag{10}$$

$$\tan(-\theta^{\Delta})\left(\left(t^R_{ij} + tz^{*I}_{ij}\left(\frac{b^c_{ij}}{2}\right)\right)\frac{w_i}{t^2_{ij}} - tz^{*R}_{ij}p_{ij} + tz^{*I}_{ij}q_{ij}\right)$$

$$\leqslant \left(t^I{}_{ij} - tz^{*R}{}_{ij}\left(\frac{b^c_{ij}}{2}\right)\right)\frac{w_i}{t^2_{ij}} - tz^{*R}_{ij}q_{ij} - tz^{*I}_{ij}p_{ij} \tag{11}$$

$$\tan(\theta^{\Delta})\left(\left(t^{*R}_{ij} + tz^{*I}_{ij}\left(\frac{b^c_{ij}}{2}\right)\right)\frac{w_i}{t^2_{ij}} - tz^{*R}_{ij}p_{ij} + tz^{*I}_{ij}q_{ij}\right)$$

$$\geqslant \left(t^{*I}_{ij} - tz^{*R}_{ij}\left(\frac{b^c_{ij}}{2}\right)\right)\frac{w_i}{t^2_{ij}} - tz^{*R}_{ij}q_{ij} - tz^{*I}_{ij}p_{ij} \tag{12}$$

B. Point of Common Coupling

$$p_{PCC} - g^s_1 w_1 = \sum_{(1,j)\in E\cup E^R} p_{1j} \tag{13}$$

$$q_{PCC} + b^s_1 w_1 = \sum_{(1,j)\in E\cup E^R} q_{1j} \tag{14}$$

$$w_1 = v^2_{PCC} \tag{15}$$

$$q_{PCC} + q^+_{mis} - q^-_{mis} = q^{set}_{PCC} \tag{16}$$

$$q^+_{mis} \leqslant \mu M \tag{17}$$

$$q^-_{mis} \leqslant (1-\mu)M \tag{18}$$

$$\sum_{k\in\{1,\ldots,n_{banks}\}} \sigma^k = 1 \tag{19}$$

$$-(1-\sigma^k)M \leqslant q^g_2 + b^k_{bank}w_i - \sum_{(2,j)\in E\cup E^R} q_{2j} \leqslant (1-\sigma^k)M \tag{20}$$

C. On Load Tap Changer

$$\sum_{k\in\{1,\ldots,n_{taps}\}} \tau^k = 1 \tag{21}$$

$$-(1-\tau^k)M \leqslant p_{ij} + p_{ji}$$
$$-r^k_{s,OLTC}\left(l_{ij} + b^c_{ij}q_{ij} + \left(\frac{b^c_{ij}}{2}\right)^2 \frac{w_i}{t^2_{ij}}\right) \leqslant (1-\tau^k)M \tag{22}$$

$$-(1-\tau^k)M \leqslant q_{ij} + q_{ji}$$
$$-x^k_{s,OLTC}\left(l_{ij} + b^c_{ij}q_{ij} + \left(\frac{b^c_{ij}}{2}\right)^2 \frac{w_i}{t^2_{ij}}\right) + \frac{b^c_{ij}}{2}\left(\frac{w_i}{t^2_{ij}} + w_j\right)$$
$$\leqslant (1-\tau^k)M \tag{23}$$

$$-(1-\tau^k)M \leqslant \left(1 - x_{ij}b^c_{ij}\right)\frac{w_i}{t^2_{ij}} - w_j$$
$$-2(p_{ij}r^k_{s,OLTC} + q_{ij}x^k_{s,OLTC})$$
$$+\left({r^k_{s,OLTC}}^2{}_{ij} + {x^k_{s,OLTC}}^2{}_{ij}\right)\left(l_{ij} + b^c_{ij}q_{ij} + \left(\frac{b^c_{ij}}{2}\right)^2 \frac{w_i}{t^2_{ij}}\right)$$
$$\leqslant (1-\tau^k)M \tag{24}$$

$$p^2_{12} + q^2_{12} \leqslant \frac{w_1}{{t^k_{OLTC}}^2} l_{12} + (1-\tau^k)M \tag{25}$$

D. Accuracy of the SOC relaxation under multi-objective optimization

The relaxation of $p^2_{ij} + q^2_{ij} = \frac{w_i}{t^2_{ij}} l_{ij}$ to an inequality means that l_{ij} could be higher than it should be in reality. However, as the losses increase with l_{ij}, the solver should not find it advantageous to have artificially larger currents and the right-hand term of Eq. (9) should reach its lower bound, i.e. the value of the left-hand term. Nonetheless, as the objective also includes the minimization of the reactive power mismatch, it could be conflicting with the loss minimization

objective and currents might take artificially larger values than they should, hence making the relaxation inexact. In practice, this is observed in some cases that will be illustrated in the following section. Artificially large currents impacts the reactive production/consumption of the wind farm. On one side, they artificially increase reactive losses on the series reactance of the lines, hence helping the wind farm to absorb reactive power. On the other side, when WTs are consuming active power (no wind, auxiliary consumption), the voltage profile decreases towards the WTs and higher currents will cause larger voltage drops towards the WTs, hence lower voltages on line charging capacitances and reduced reactive power production from these elements. This analysis is valid when the voltage at the secondary of the collector transformer is constant. However, the OLTC can adapt this voltage hence the observed behaviour might differ from what has been described here.

E. Linear outer approximation of second order cone constraints

The model presented above is a mixed-integer second order cone program. We further relax it with a linear outer approximation of conic constraints. As a matter of fact, a large amount of instances of the problem have to be solved in order to cover the range of different operating conditions encountered throughout a year in the windfarm. Yet, the state-of-the-art Mixed-Integer Quadratically Constrained (MIQCP) solvers are not as mature as the mixed-integer linear programming solvers (MILP) [7], which is reflected on the computation time. Hence we use a linear outer relaxation of the conic constraints initially developed by Ben-Tal and Nemirovski in [8] and further analyzed in [9], which is abbreviated BTN hereafter. This lift-and-project relaxation approximates a three-dimensional second order cone, generically denoted by $\mathbb{L}^2 = \{(x, y, z) \in \mathbb{R}^3 | x^2 + y^2 \leqslant z^2\}$, with a polyhedron $\mathcal{L}^\kappa$ in the lifted space $\mathbb{R}^{2\kappa+3}$. This relaxation, characterized by its degree κ is defined hereunder as in [9]:

BTN relaxation: linear outer approximation of $\mathbb{L}^2$ with $\mathcal{L}^\kappa$

$$\mathcal{L}^\kappa = \{(z, \alpha_0, \beta_0, ..., \alpha_\kappa, \beta_\kappa) \in \mathbb{R}^{2\kappa+3}\}$$

s.t.

$$\begin{cases} \alpha_0 = x \\ \beta_0 = y \end{cases}$$

$$\begin{cases} \alpha_{i+1} = \alpha_i \cos\frac{\pi}{2^i} + \beta_i \sin\frac{\pi}{2^i} \\ \beta_{i+1} \geqslant \beta_i \cos\frac{\pi}{2^i} - \alpha_i \sin\frac{\pi}{2^i} \\ \beta_{i+1} \leqslant \beta_i \cos\frac{\pi}{2^i} - \alpha_i \sin\frac{\pi}{2^i} \\ z = \alpha_\kappa \cos\frac{\pi}{2^\kappa} + \beta_\kappa \sin\frac{\pi}{2^\kappa} \end{cases} \quad \forall 0 \leqslant i \leqslant \kappa$$

The BTN relaxation, illustrated on Fig. 4, is an ϵ^M-approximation of SOC constraints in the sense that $||(x, y)|| \leqslant (1 + \epsilon^M)z$ with $\epsilon^M = \cos(\pi/2^{\kappa+1})^{-1}$ the largest possible error of the relaxation as shown in [8]. As

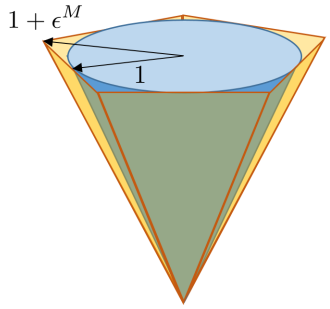


Fig. 4. BTN Linear Outer Approximation (yellow) of the second order cone (blue)

ϵ^M decreases exponentially with the relaxation degree κ, a reasonably small degree should be sufficient in order to reach a satisfying level of accuracy. In the particular case of the BTN relaxation of (9), the observed ϵ will imply that the product of squared voltage and current amplitudes could be underestimated, in turn causing an underestimation of losses. The physical interpretation for this is that the estimation of losses may be overoptimistic compared to what the losses should be with respect to active and reactive power flow constitutive equations.

IV. Numerical results

A. Accuracy of the relaxation

The solution s to the relaxed problem presented in the previous section is considered to be the combination of setpoints for the OLTC, bus voltages and reactive power production/consumption of WTs and static units, i.e. $s = (q^g, \sqrt{w}, \sigma, \tau)$. As explained in the previous section, the SOC relaxation is exact in this radial case if and only if (9) is satisfied with equality. Let us define the relative relaxation error $\epsilon_{ij} \in \mathbb{R}\ \forall\ (i, j) \in E \cup E^R$ as follows:

$$||(p_{ij}, q_{ij})|| = \sqrt{p_{ij}^2 + q_{ij}^2} = (1 + \epsilon_{ij})\sqrt{\frac{w_i}{t_{ij}^2} l_{ij}}$$

It has been shown that the additional BTN relaxation allowed the right-hand term of (9) to be underestimated, i.e. $\epsilon_{i,j} > 0$. Furthermore, as explained in the previous section, with potentially conflicting objectives, the right-hand term of (9) might be overestimated as well, i.e. $\epsilon_{ij} < 0$. This is illustrated on Fig. 5. Let us further define the maximal error $\bar{\epsilon}$ as

$$\bar{\epsilon} = \{\epsilon_{ij} \text{ with } (i, j) \text{ s.t. } |\epsilon_{ij}| = \max_{(i,j)} |\epsilon_{ij}|\}$$

A solution from the BTN relaxation of the model will be considered accurate under the following conditions:

(i) The observed $\bar{\epsilon}$ is sufficiently small
(ii) The solution is feasible. This is determined by running a Power Flow problem (PF) with *Matpower* using s as an input.

Note that this is not the mathematical definition of feasibility. For the relaxation solution to be mathematically feasible,

$\underset{\sim}{q^g}, \underset{\sim}{\sigma}, \underset{\sim}{\tau}, \underset{\sim}{p_{ij}}, \underset{\sim}{q_{ij}}$ should satisfy power flow equations exactly which will obviously not be the case because power flows are affected by the relaxation inaccuracies. This is compensated by the fact that the PCC is the slack bus in the PF problem. Active and reactive power injections at this bus thus serve as adjustment variables that compensate for those inaccuracies. Hence, the PF gives the exact value of p_{PCC} that would be obtained if the solution $s = (\underset{\sim}{q^g}, \sqrt{\underset{\sim}{w}}, \underset{\sim}{\sigma}, \underset{\sim}{\tau})$ of the relaxed problem was implemented in the wind farm. For the purpose of testing the accuracy of the relaxations, 6 test-cases are defined according to the active power production (P) of the wind farm, whether it should absorb or inject reactive power (Q) from/to the transmission network and whether or not a mismatch is foreseen between the wind farm reactive setpoint and its effective reactive power output. The latter element determines whether there are two conflicting objectives or not, which has to be investigated regarding the accuracy of the SOC relaxation, as mentioned in the previous section. Those are considered to be limit cases representing the various extreme configurations that could be encountered in the operation of this wind farm:

Case 1. P: high, Q: consumption, no expected mismatch
Case 2. P: high, Q: consumption, expected mismatch
Case 3. P: low, Q: consumption, expected mismatch
Case 4. P: high, Q: injection, no expected mismatch
Case 5. P: high, Q: injection, expected mismatch
Case 6. P: low, Q: injection, expected mismatch

The results for theses 6 cases are shown in table I. First, it can be observed that for cases 1 and 4, when no reactive mismatch is foreseen, the relaxed problem gets more and more accurate as κ grows. A value of 10 for this relaxation parameter allows to reach a satisfying precision of 3.3×10^{-3} and 2×10^{-4} for cases 1 and 4 respectively. Hence, in these cases, the relaxation can be made to arbitrary accuracy by increasing κ at the cost of a higher computational burden. For cases 2 and 3, the accuracy of the relaxation does not improve with κ and ϵ is even negative. This is due to the fact that the wind farm is supposed to absorb a higher amount of reactive power than it is capable of and there is a reactive mismatch which is penalized in the objective function. To reduce this mismatch and the objective value, the solver finds it advantageous to give larger values to currents in order to cause artificial reactive losses on the collector grid of the wind farm as explained in the previous section, even though active losses are also increased.
A mismatch is also expected in case 6. However, since the wind farm is absorbing active power, artificially large currents cannot help to reach the reactive injection setpoint, hence the relaxation is observed to be increasingly accurate with κ. Finally, the relaxed problem may not be considered accurate in case 5 as the relaxation error is not decreasing at it should. Indeed, currents were expected to be as small as possible to decrease line reactive losses, hence better following the reactive injection setpoint. This is not what is observed as the relaxation error does not decrease with κ. We may thus conclude that the relaxed problem delivers accurate solutions when there is no foreseen reactive mismatch and might give poorer results when there is a reactive mismatch.

TABLE I
ACCURACY AND FEASIBILITY OF THE RELAXATION FOR 6 TEST CASES

Case	Total production [MW]	Reactive setpoint [MVar]	κ	$\bar{\epsilon}$	Feasible
1	78	12	6	8.7×10^{-2}	yes
			8	1.8×10^{-2}	yes
			10	3.5×10^{-3}	yes
			12	3.3×10^{-5}	yes
2	78	100	6	-8.2×10^{-1}	yes
			8	-7.3×10^{-1}	yes
			10	-9.7×10^{-1}	yes
			12	-9.8×10^{-1}	yes
3	-0.2	100	6	∞	yes
			8	-6.1×10^{-1}	yes
			10	-6.1×10^{-1}	yes
			12	-6.1×10^{-1}	yes
4	78	-12	6	1.1×10^{-1}	yes
			8	3.4×10^{-2}	yes
			10	2×10^{-4}	yes
			12	2.8×10^{-4}	yes
5	78	-100	6	1.9×10^{-1}	yes
			8	8.1×10^{-2}	yes
			10	-9.9×10^{1}	yes
			12	-9.9×10^{1}	yes
6	-0.2	-100	6	∞	yes
			8	1.5×10^{-1}	yes
			10	5.5×10^{-3}	yes
			12	1×10^{-4}	yes

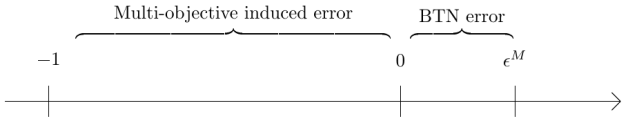


Fig. 5. Error introduced by the BTN linear outer approximation and the multi-objective character

B. Comparison with a Matpower-based approach

In this section, the goal is to compare the results obtained with the relaxed model to those obtained on the exact, non-linear model with *Matpower* using MIPS (*Matpower* Interior Point Solver). *Matpower* does not provide tools to include elements such as the static units and the OLTC that are characterized by binary variables. For this reason, external loops are used to solve the OPF in each of the 147 configurations corresponding to the 21 taps of the OLTC and the 7 states of the static units. Real data originating from the wind farm covers the whole year 2014 on a 10 min basis. This represents 52560 timesteps. In order to alleviate the computational burden, these data have been clustered into 100 fictitious timesteps with the k-means algorithm. The goal of the comparison is to see if the solution of the relaxed problem might be better than that of the exact one, i.e. if p_{PCC} is smaller in the former case (recall that $p_{PCC} < 0$ if injected

on the grid).

As mentioned in the previous section, a solution s of the relaxed model is injected in a *Matpower* PF to check its feasibility and the exact power output of the wind farm. To assess the accuracy of the relaxed model in terms of results, we also compute the difference between active and reactive power injections at the PCC in the solution of the exact problem and in the solution of the relaxed one. A smaller difference means a lesser slack compensation, hence lesser inaccuracies on power flows in the relaxed model. The performance of the relaxed model compared to the exact one is presented in Fig. 6 where the objective improvement is plotted against the accuracy of the relaxed model for several degrees κ of the BTN relaxation. Negative ordinates represent situations where the solution of the relaxed problem gives a better objective than the one from the exact problem. In physical terms, this means that the losses on the collector grid are lower in the relaxed model solution than in the *Matpower* solution. Several observations can be made about this graph. First, it can be seen that a higher accuracy is obtained by increasing κ, which was already shown on extreme cases from the previous section. Then, it can be observed that the relaxed model outperforms the *Matpower*-based approach on a significant fraction of cases, roughly ranging from 10% to 25% when κ goes from 8 to 12. Finally, we can see that the points where the relaxed model performs significantly worse or better than the exact one are the ones with the lowest accuracy $\forall\kappa$. This result seems counterintuitive and needs further investigation to be explained.

It can be concluded from these results that *Matpower* sometimes falls in local minima, as it is expected from nonconvex problems, since the relaxed model is able to find better solutions in some cases, i.e. solutions with lower losses. We also compare the results based on the computation time for the different models. As it can be seen on Fig. 7, the relaxed model is faster to solve than the exact one for most cases for $\kappa = 8$. However, this is not the case anymore for $\kappa = 10$ and 12 as the computation time increases by up to one and two orders of magnitude respectively.

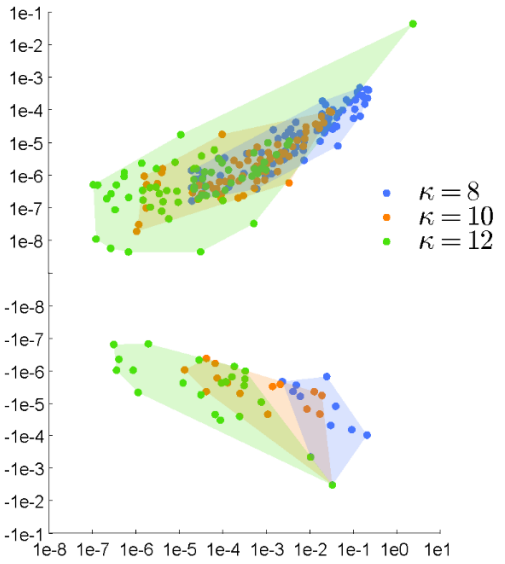


Fig. 6. Comparison of performances of the exact model and the relaxed models. X-axis: $|\Delta P_{slackBus,PF}| + |\Delta Q_{slackBus,PF}|[MVA]$ Y-axis: $|P_{PCC,exact}| - |P_{PCC,rel}|[MW]$

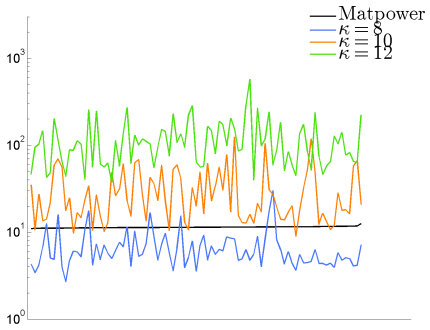


Fig. 7. Computation time $[s]$ for the different fictitious points and models

V. Conclusion

In this paper, we presented an extended convex DistFlow relaxation of the OPF problem able to cope with real-world network elements such as OLTC and capacitive cables. This relaxation is first formulated as a MISOCP and then further relaxed into a more tractable MILP, using an efficient outer approximation that can be made arbitrarily accurate (at the price of an increase in size of the model). This relaxed model is exact or close to exact in many situations. However, when the two components in its objective function are conflicting with each other, i.e. active loss minimization and compliance with a reactive setpoint, the relaxed model's performance is degraded. Nonetheless, this model already outperforms the *Matpower*-based approach on a significant fraction of test cases, in terms of objective value and computation time, and it is expected that the relaxed model becomes more advantageous for instances including more discrete variables. Finally, it has been observed that the performance of our model is either significantly worse or better than *Matpower* when the accuracy of the relaxed problem is lower. This counterintuitive result has not been explained yet and requires further testing for a better understanding of such a behavior.

Acknowledgements

The first author is supported by a FRIA grant from the Belgian Fund for Scientific Research - FNRS. He would like to thank warmly C. Coffrin from Los Alamos National Laboratory for the precious explanations about the DistFlow formulation, the support regarding convex optimization and the proofreading of this paper. The last author acknowledges support from the Concerted Research Action (ARC) programme by the Federation Wallonia-Brussels (contract ARC 14/19-060).

REFERENCES

[1] K. Lehmann, A. Grastien, and P. V. Hentenryck, "AC-Feasibility on Tree Networks is NP-Hard," *IEEE Transactions on Power Systems*, vol. 31, pp. 798–801, Jan. 2016.

[2] D. K. Molzahn and I. A. Hiskens, "A Survey of Relaxations and Approximations of the Power Flow Equations." invited submission to *Foundations and Trends in Electric Energy Systems*.

[3] L. Gan and S. H. Low, "Convex relaxations and linear approximation for optimal power flow in multiphase radial networks," in *Power Systems Computation Conference (PSCC), 2014*, pp. 1–9, IEEE, 2014.

[4] M. Nick, R. Cherkaoui, J.-Y. LeBoudec, and M. Paolone, "An Exact Convex Formulation of the Optimal Power Flow in Radial Distribution Networks Including Transverse Components," *IEEE Transactions on Automatic Control*, 2017.

[5] C. Coffrin, H. L. Hijazi, and P. Van Hentenryck, "DistFlow Extensions for AC Transmission Systems," *arXiv:1506.04773 [cs, math]*, May 2015. arXiv: 1506.04773.

[6] R. D. Zimmerman, C. E. Murillo-Sanchez, and R. J. Thomas, "MATPOWER: Steady-State Operations, Planning, and Analysis Tools for Power Systems Research and Education," *IEEE Transactions on Power Systems*, vol. 26, pp. 12–19, Feb. 2011.

[7] S. Mhanna, G. Verbic, and A. Chapman, "Tight LP Approximations for the Optimal Power Flow Problem," *arXiv preprint arXiv:1603.00773*, 2016.

[8] A. Ben-Tal and A. Nemirovski, "On polyhedral approximations of the second-order cone," *Mathematics of Operations Research*, vol. 26, no. 2, pp. 193–205, 2001.

[9] F. Glineur, *Topics in Convex Optimization: Interior-Point Methods, Conic Duality and Approximations*. PhD thesis, Facult Polytechnique de Mons, 2001.